Construction of a low velocity metastable Helium atomic beam

G.R. Woestenenk, J.W. Thomsen, M. van Rijnbach, P. van der Straten, and A. Niehaus
Debye Institute, Department of Atomic- and Interface Physics - Utrecht University
P. O. Box 80.000, 3508 TA Utrecht, The Netherlands
(submitted)

We have constructed an atomic beam of metastable helium atoms He(2^3S) with a mean velocity of 300 m/s (15 K) and a yield of 3×10^{12} atoms/s sr. The metastable atoms are produced in a DC-discharge in a cryogenic environment cooled by liquid helium. Using a hexapole magnetic lens we have increased further the beam intensity by focusing the metastable atoms. Initial studies show a factor of 2.5 increase in the beam flux but more is expected when the hexapole is constructed from permanent hexapole magnets. The He(2^3S) atoms are subsequently loaded into a magneto-optical trap (MOT).

I. INTRODUCTION

Since the development of laser cooling and trapping of atoms [1], studies with low temperature atoms have increased dramatically. Areas of interest include Bose-Einstein Condensation [2], high precision spectroscopy [3], and quantum optics [4]. One of the main tools in these experiments is the magneto-optical trap (MOT). Among the elements that are studied the metastable rare gases play an important role [5–7].

For experiments using ultra-cold atoms it is important to have an intense source of atoms with a low velocity. Typical capture velocities for MOT's lie around 60 m/s. In order to trap atoms with high initial velocities, *e.g.* metastables that are produced in a discharge, the atoms need to be pre-cooled in a Zeeman slower. This makes the experiment more complicated and the loading of the MOT less efficient. Therefore it is desirable to be able to load a MOT efficiently from a source without using any pre-cooling schemes.

This paper demonstrates the production of an intense low velocity metastable helium beam suitable for loading a MOT without a Zeeman slower. Furthermore, we have also constructed a magnetic hexapole lens, that can efficiently focus the atomic beam.

II. CONSTRUCTION

The source is shown schematically in Fig. 1. Metastable helium atoms He(2^1S) and He(2^3S) are produced in a DC discharge by electron impact. The source is cooled by liquid helium. The discharge runs between a discharge needle and a nozzle plate. A Pyrex glass tube with an orifice of 1 mm inserted in a Teflon holder, is placed in a copper assembly as shown in Fig. 1. The gas flows on the outside of the glass tube, along the cold cryostat and cold nozzle before it expands into the vacuum chamber. Part of the gas is pumped out by a mechanical pump through the glass tube, as in the liquid-nitrogen-cooled DC-discharge source described by Kawanaka *et al.* [8].

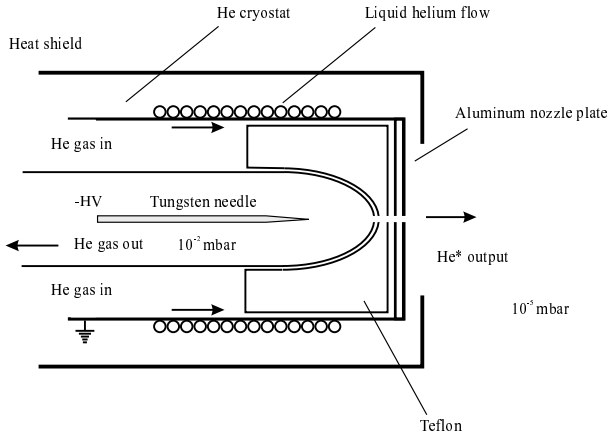

FIG. 1. Schematic drawing of the source cooled by liquid helium.

The glass tube and nozzle assembly were placed inside a cryostat, which was cooled to about 10-15 K by liquid helium. Lower temperatures could be obtained but at the expense of instability of the source output. This is possibly due to helium condensation taking place in the source. The cryostat is heat shielded by a gold plated cylinder. The nozzle was made of an aluminum plate of 1 mm thickness to reduce heat gradients (a copper nozzle did not perform as well as an aluminum one) and the exit hole diameter used was 0.5 mm. As a discharge needle we used a tungsten rod with a diameter of 2 mm, which was sharpened at the end and kept in the middle of the glass tube by ceramic spacers. The optimal distance from the nozzle plate to the discharge needle was found to be 7 mm, ensuring both a high output stability and a high yield of the source. To minimize heating effects the source is operated at a low discharge power of typically 50-100 mW (about 0.1 mA) and a low discharge pressure of 10^{-2} mBar.

The helium discharge is localized inside the source, *i.e.* between the discharge needle and the nozzle plate. This is in contrast to conventional metastable sources which operate at higher pressures (a few mBar) with a discharge burning outside the nozzle, *i.e.* between the discharge needle and the skimmer, to reduce quenching of the metastable atoms [9,10]. We observed that such operation was only possible at higher source pressures and currents, and therefore at higher temperatures. However, we estimated the quenching of the metasta-

bles in our design to be of minor importance due to our low source pressure of 10^{-2} mBar. Operating at minimum power and pressure yields a total flux of a few times 10^{12} atoms/s sr. This output is two orders of magnitude lower than that of conventional sources, but the mean velocity of the atoms is decreased from 2000 m/s to 300 m/s, as is shown in Sec. III. As expected, higher source voltages increase the output yield further. This effect is illustrated in Fig. 2.

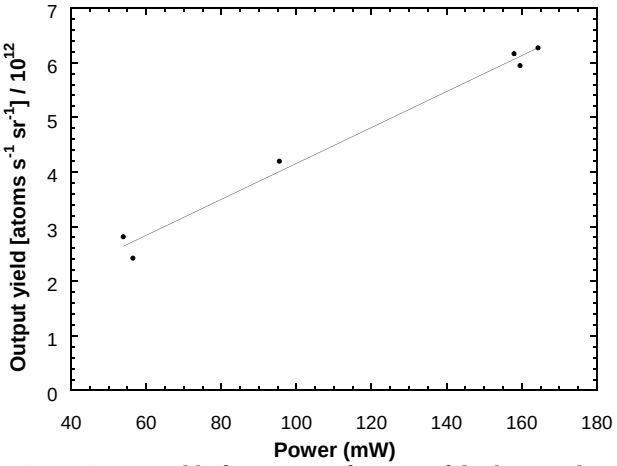

FIG. 2. Output yield of source as a function of discharge voltage. The contribution from UV photons has been subtracted.

III. RESULTS

In the source He(2^3S) atoms, He(2^1S) atoms, and UV photons are produced. The atoms and the photons were detected with a channeltron detector, located 60.3 cm away from the source exit. The total number of UV photons in the beam was deduced from time of flight (TOF) measurements discussed below and subtracted from the signal measured with the channeltron detector. The fraction of He(2^1S) atoms produced in the source was measured by deflecting all He(2^3S) atoms out of the beam with a diode laser resonant with the He($2^3S_1 \rightarrow 2^3P_2$) transition. The beam flux was measured with and without deflection, which enabled us to determine the number of singlet atoms. The fraction of singlet atoms was found to be 5–8% of the total beam flux which is rather low compared to previous source designs [10].

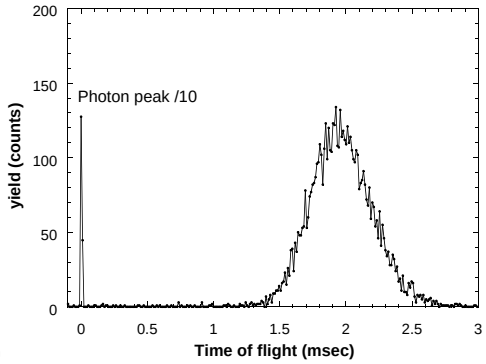

(a)

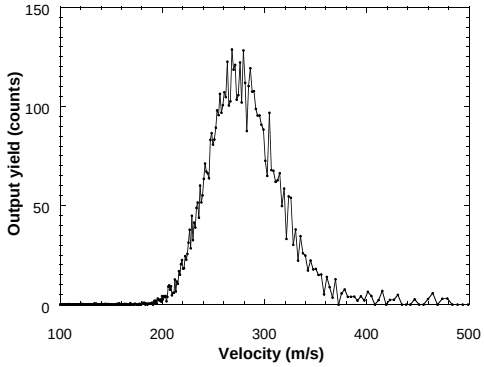

(b)

FIG. 3. Part (a) shows a typical time of flight spectrum obtained using a mechanical chopper. A channeltron detector located 60.3 cm away from the chopper monitored the beam particles and photons. Part (b) displays the corresponding velocity distribution.

The velocity distribution was measured by a TOF technique. Fig. 3 shows a typical TOF spectrum together with the corresponding velocity distribution. The TOF spectrum was obtained by use of a mechanical chopper inserted in the beam. The sharp photon peak at the beginning of the spectrum provided a convenient time zero as well as an indication of the time resolution in this measurement, which was estimated to be better than 2 μs. Furthermore, we used the photon peak to determine the photon flux, which is approximately 25% of the total source output. The mean velocity of the spectrum shown in Fig. 3 is 300 m/s, which corresponds to a temperature of 15 K. In Fig. 4 the mean metastable atom velocity is plotted against discharge power. As the discharge power increases the mean velocity increases slightly, due to heating of the discharge. At typical settings of the source we find a mean velocity of less than 300 m/s, compared to 1000 m/s for a liquid nitrogen cooled source [8], or 2000 m/s for a conventional source [9,10].

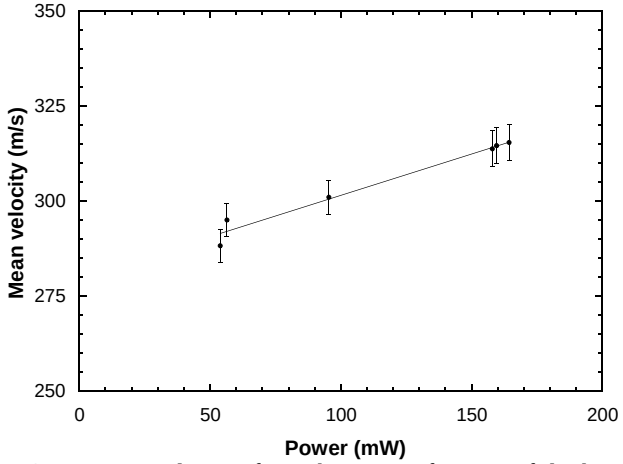

FIG. 4. Mean velocity of He* beam as a function of discharge power.

IV. LOADING THE MOT

Our source of slow He(2^3S) atoms is used to load a magneto-optical trap (MOT). A schematic picture of the setup is shown in Fig. 5. Usually a He(2^3S) MOT is loaded from a high-pressure discharge source cooled with liquid nitrogen [6,11–13]. Here the atoms need to be slowed in a Zeeman slower from 1000 m/s to typically 60 m/s, before they can be captured in the MOT. Using a Zeeman slower makes the experiment more complex since special care has to be taken to avoid reduction of density of the beam [14]. In a Zeeman magnet the beam is slowed down in the longitudinal direction and as it is slowed down, the transverse part of the velocity becomes more and more dominant. The beam will ultimately fan out and the flux in the center of the beam will strongly decrease. This effect limits the number of atoms that can be captured in the MOT. It can be compensated for by inserting a transverse cooling section in front of and/or at the end of the slowing unit [11]. At the entrance of the slower the velocity of the atoms in the beam is high and consequently the interaction time of cooling light with the atoms is short. This limits the momentum that can be transferred to the atoms. A complication that arises when using a Zeeman slower is extraction of slow atoms from the end of the slower. The extraction can be made more efficient by placing additional coils at the exit of the magnet, or by using an increasing magnetic field [15]. These modifications also prevent further deceleration of the beam and broadening of the velocity distribution after the atoms have left the slower.

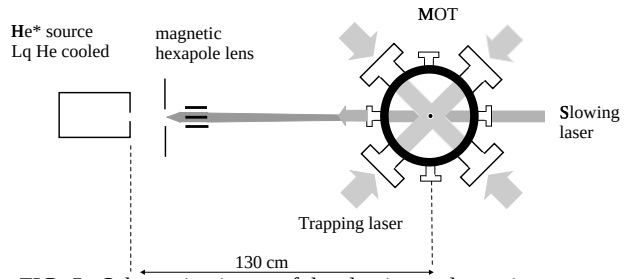

FIG. 5. Schematic picture of the slowing and trapping setup.

To improve the load characteristics of our He* MOT compared to previous experiments [16], we decided to use a cryogenic helium source instead of a source cooled with liquid nitrogen. Since the mean velocity is only 300 m/s instead of 1000 m/s, we could decrease the length of the experiment considerably and hence increase the loading rate dramatically. The coils that generate the MOT magnetic field in our setup are large in diameter ($\sim$ 400 mm). These large coils are particularly favorable for loading a MOT from the cryogenic source, since no additional Zeeman slower is needed. The atoms are slowed down by a counter propagating laser beam, and the Zeeman shift that is needed to compensate the Doppler shift is produced by the radial magnetic field of the MOT. The beam still fans out, but the effect is smaller than for a liquid nitrogen cooled beam for two reasons. First, due to the lower initial velocity of the atoms the beam does not spread out as much during the deceleration. Second, since the atoms are slowed down in the MOT chamber the beam spreads out most in the region where the trapping laser beams are present. This reduces the losses considerably. Fig. 6 shows a simulation of the slowing in the radial MOT magnetic field by a single counter-propagating laser. As a reference we have also plotted the measured and calculated radial magnetic field. The detuning and intensity of the slowing laser that are used in the simulation are identical to the values that are used in the actual experiment, which are given below.

For a slowing laser detuned 40 MHz below the He($2^3S_1 \rightarrow 2^3P_2$) transition asymptote with a saturation parameter of $s_0 = 400$ we are able to slow down all atoms with a velocity that is less than 325 m/s, *i.e.* most of velocity distribution. Experiments show that it is indeed possible to trap most of the atoms from the slow metastable helium beam. We easily trap about 10^6 atoms in the MOT, where in the previous experiment only 10^5 atoms were trapped by loading the MOT from a liquid nitrogen cooled Zeeman slowed beam [16]. The volume is 1 mm^3 leading to an average density of a few times 10^9 cm^{-3} and the temperature is 1 mK. The total number of trapped atoms is measured with micro-channel plates and the spatial size of the MOT is measured by a CCD camera. With this number and density of atoms we have entered the regime where intra-MOT collisions are more important than collisions with background atoms. This can clearly be seen in Fig. 7 where a typical decay curve of the MOT is shown. Since the decay is not a single exponential in time, the main ion production results from intra-MOT collisions [17].

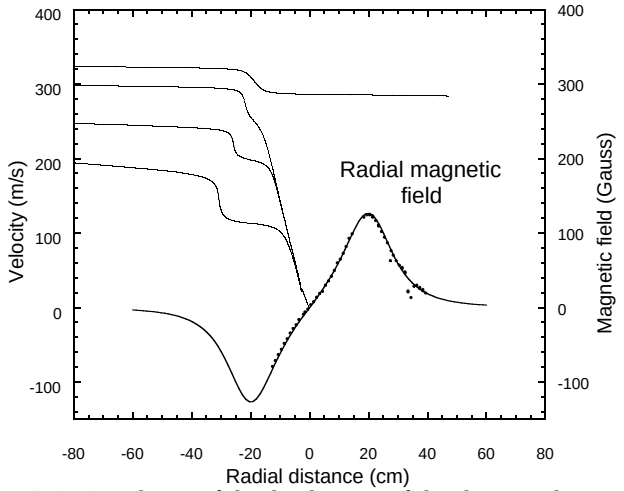

FIG. 6. Simulation of the deceleration of the slow He* beam in the radial magnetic field of the MOT. For reference we have also added the radial magnetic field component on the graph. The dots are measured magnetic field values. The beam of He* atoms enters the MOT chamber at the negative radial distance side. The simulation is shown for various initial velocities of the atoms. It can be seen that atoms with a velocity smaller than 325 m/s can be slowed down enough to be trapped in the MOT.

V. HEXAPOLE MAGNETIC LENS

The slow metastable helium source offers the possibility of manipulating the beam profile with magnetic fields. At low atomic velocities moderate magnetic field gradients are sufficient to reduce the initial beam divergence and to project a larger part of the flux into the capture region of the MOT. This can result in a significant increase in the number of captured atoms. The best way to accomplish this is to use a magnetic hexapole lens to focus the He* atoms. In Fig. 5 the position of the magnetic lens is shown and in Fig. 8 a schematic picture of the hexapole lens can be seen. We have chosen a hexapole configuration which produces a field gradient that increases linearly with the distance from the center of the hexapole. Metastable atoms with a large divergence thus experience a larger force than atoms with a small divergence and in principle all atoms will be focused to the same point. This is in contrast to a quadrupole configuration where the gradient is constant as a function of distance. The hexapole thus resembles a lens for mono-velocity atoms. However, in our case the atoms in the beam have a velocity spread and velocity aberration can be important.

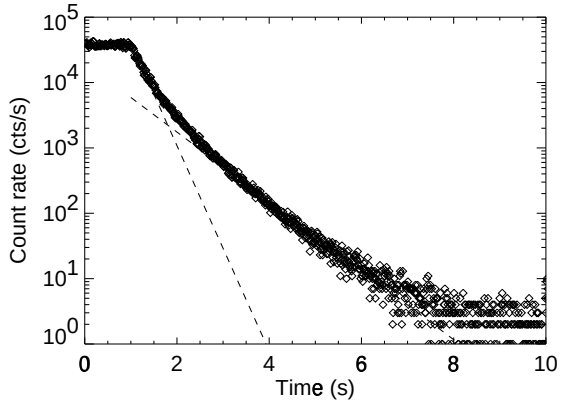

FIG. 7. Decay curve of the MOT. The loading of the MOT is shut off at t = 1.0 s. The two dashed lines represent the contributions to the decay rate of intra-MOT collisions (steep slope) and of collisions with background atoms (weak slope).

The hexapole is constructed from a tube of copper with a length of 40 mm, an inner diameter of $d_{\rm in}$= 2.6 mm and an outer diameter of $d_{\rm out}$= 5 mm. The hexapole structure is obtained by cutting 6 slots in the copper tube along its side with a spark cutter such that six wire segments are created (see Fig. 8). At each end of the tube 2 neighboring segments remain connected to each other such that the current is allowed to flow alternately in opposite directions. The tube assembly is connected to two wires supplying the current. The distance between each wire segment of the hexapole is about one millimeter. A ceramic tube with an inner diameter of 1.6 mm inside the hexapole lens ensures that the segments remain fixed at their positions, avoiding unwanted contact between the segments. Our hexapole structure can take a continuous current of about 15-20 A, without cooling, and a maximum of 80 A for a short period of time. At high currents the surroundings of the lens warm up, leading to an increase in pressure by outgassing and a corresponding quenching of the metastables. Since our hexapole is most efficient at higher currents we plan to use permanent magnets in the future.

We have modeled the atom trajectories and kinematics through the lens. We assume that the magnetic field is generated by six infinite point wires put at a distance a from the center of the hexapole. To test this assumption we have carried out numerical simulations of the actual field and compared it to our analytical results, which will be discussed below, and found that the distance a is just the average of the inner radius $a_{\rm in} = d_{\rm in}/2$ and the outer radius $a_{\rm out} = d_{\rm out}/2$, or $a = (a_{\rm in}+a_{\rm out})/2$. For six point wires we obtain in cylindrical coordinates (r, θ) for the magnetic field:

$$B(r,\theta) = \left(\frac{\mu_0}{4\pi}\right)\frac{12Ir^2}{a^3}\frac{1}{\sqrt{1+\left(\frac{r}{a}\right)^{12}-2\left(\frac{r}{a}\right)^6\cos(6\theta)}}, \quad (1)$$

where I is the current sent through each wires. This expression is exact for all points (r, θ) in the plane. For small $r \ll a$ we obtain

$$B(r,\theta) = \left(\frac{\mu_0}{4\pi}\right)\frac{12Ir^2}{a^3}, \quad (2)$$

which we find to be valid for $r \leq a/2$. Note that the field depends quadratically on the radius r and thus that the gradient is linearly proportional to the radius. Therefore the hexapole field provides the right field for an atomic lens. For a quadrupole configuration we obtain an r/a^2 dependence of the field, which does not yield the right dependence for a lens. The interaction between the atom and the magnetic field is given by the Zeeman shift:

$$V = \mu_b g_s m_j B, \quad (3)$$

where μ_b is the Bohr magneton, g_s is the spin gyromagnetic ratio, and m_j is the projection of the total electronic angular momentum along the r direction. The force on the atom is given by:

$$F(r) = -\mathrm{grad}V = -\mu_B g_s m_j \frac{\partial B}{\partial r} = -\kappa r, \quad (4)$$

with the spring constant κ given by

$$\kappa = \mu_B g_s m_j \left(\frac{\mu_0}{4\pi}\right)\frac{24I}{a^3}. \quad (5)$$

We assume the m_j distribution to be random, since the atoms move too fast through the lens for adiabatic following to take place. Thus along the r direction one third of the metastables will be in each of the states $m_j = 0, \pm 1$. Atoms in the $m_j = +1$ state will be deflected towards the axis of the hexapole, atoms in the $m_j = 0$ state will not experience any influence, while atoms in the $m_j = -1$ state will be deflected away from the axis.

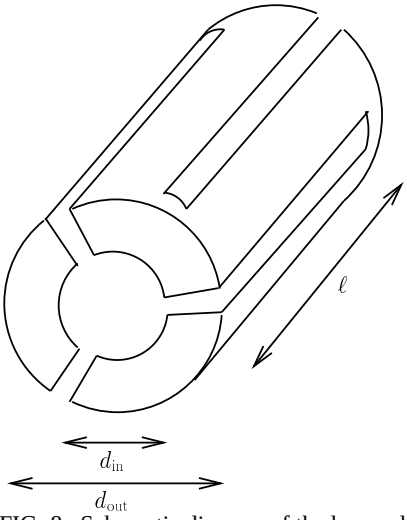

FIG. 8. Schematic diagram of the hexapole lens. The inner diameter of the tube is $d_{\rm in}$=2.6 mm, the outer diameter $d_{\rm out}$= 5 mm and the length ℓ= 40 mm. Note, that due to the special arrangement of the slots the direction of the current alternates between two adjacent segments.

In the hexapole the atoms will undergo an oscillatory motion. If the interaction time $\tau = \ell/v_0$ is small compared to the oscillation period $T = 2\pi/\omega$, where $\omega = \sqrt{\kappa/m}$ is the oscillation frequency, a parallel beam of atoms will be focused at a distance f from the lens given by

$$f = \frac{m{v_0}^2}{\kappa\ell} \tag{6}$$

and f thus represents the focal length of our lens. Here we have assumed that $\tau/T \ll 1$, *i.e.* we have made the thin lens approximation, which is not strictly valid in our case, but without this approximation we obtain equivalent results. Note, that the focal length of the lens is proportional to the square of the velocity and thus shows strong velocity aberrations. In our case, we can generate a gradient of d^2B/dr^2= 6000 G/cm^2 with a current of 20 A and for atoms with a velocity of 300 m/s we obtain a focal length of 12 cm.

In the present setup we are not interested in the focal properties of the lens, since the spread in the velocity of the atoms is too high. Instead we are interested to use the hexapole lens to boost the flux of atoms which can be loaded in the MOT. Solving the equation of motion for a given velocity and entrance coordinate in the hexapole enables us to determine the impact position in the detector plane located approximately 1.6 m away from the hexapole. In the calculation we assumed the initial beam profile to be Gaussian and the velocity distribution, depicted in Fig. 3, to be of the form

$$f(v) = Cv^3 \exp\left(-\left(\frac{v - v_0}{\Delta v}\right)^2\right), \tag{7}$$

where C is a normalization constant, v_0=300 m/s is the mean velocity and Δv= 50 m/s describes the width of the distribution. The beam profile $P(r)$ in the detector plane is obtained from

$$P(r) = \int_0^\infty A(v,r)\, f(v) dv, \tag{8}$$

where $A(v,r)$ is the beam profile transformed first by the hexapole and then by propagation to the detector plane.

We have calculated the beam profile for a number of values of the current through the hexapole, varying from I = 20 A to I = 100 A, and also measured the beam profile for various values of I. The maximum calculated flux enhancement is a factor of 12. The detector can only be scanned in one direction and might not be at the optimal position perpendicular to the scanning direction, since a small misalignment of the hexapole lens can have a large effect at the distance where the detector is placed. Therefore we have plotted the enhancement of the flux at a fixed position of the detector and used the calculation that fits the measurements the best. The measurements and the calculations are plotted in Fig. 9, where the background of UV photons and He (2^1S) atoms has been subtracted from the measured signal. It can be seen that if the current scale of the calculations is multiplied by a factor of 2, the agreement between the measurements and the calculations is rather good.

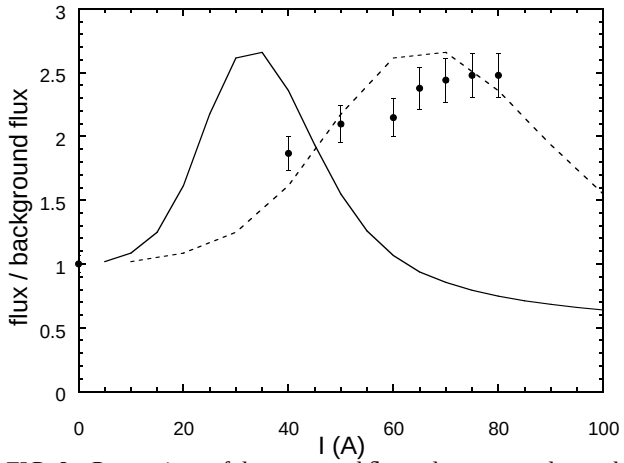

FIG. 9. Comparison of the measured flux enhancement due to the hexapole lens as a function of the current I compared to the calculated flux enhancement. The dots are the measured values, the solid line is the calculation and the dashed line is the calculation where the current scale has been multiplied by 2 to obtain better agreement with the measurements.

A few assumptions have been made in the calculations that might explain this discrepancy in the current scale. First of all, we have assumed that the He* source is a point source, while in reality the diameter of the nozzle is too large and the source is too close to the lens to be regarded as a point source. Furthermore, the atoms might spiral through the lens due to the magnetic field, since the velocity of the atoms has both a radial and a longitudinal component as a result of the finite extend of the source. Finally, we have not been able to measure the magnetic field in the hexapole, to check whether our calculations are correct.

We can conclude that we can indeed enhance the beam flux with the hexapole magnet, although not in the way we

expected. To improve the flux even more the hexapole lens should be positioned farther away from the source, so that a lens with a larger focal length should be optimal and hence lower currents could be used. Another possibility is to use permanent magnets to create the magnetic hexapole field in order to obtain higher field gradients.

ACKNOWLEDGEMENT

This work has been supported by the "Stichting voor Fundamenteel Onderzoek der Materie (FOM)", which is financially supported by the "Nederlandse organisatie voor Wetenschappelijk Onderzoek (NWO)" and JWT is supported by the European Union's TMR programme under contract number ERB4001GT95292.

---

[1] H.J. Metcalf and P. van der Straten, *Laser Cooling and Trapping*, Springer-Verlag, New York (1999).
[2] D.S. Durfee and W. Ketterlee, Opt. Expr. **2**, 299 (1998).
[3] P. D. Lett, P. S. Julienne, and W. D. Phillips, Annu. Rev. Phys. Chem. **46**, 423 (1995).
[4] J. Mlynek, V. Balykin, and P. Meystre (eds.), *Optics and Interferometry with Atoms*, Appl. Phys. B **5**, 319–485 (1992).
[5] M. Walhout, U. Sterr, C. Orzel, M. Hoogerland, and S. L. Rolston, Phys. Rev. Lett. **74**, 506 (1995).
[6] H. C. Mastwijk, J. W. Thomsen, P. van der Straten, and A. Niehaus, Phys. Rev. Lett. **80**, 5516 (1998).
[7] N. Herschbach, P.J.J. Tol, W. Vassen, W. Hogervorst, G. Woestenenk, J.W. Thomsen, P. van der Straten, and A. Niehaus, Phys. Rev. Lett. **84**, 1874 (2000).
[8] J. Kawanaka, M. Hagiuda, K. Shimizu, F. Shimizu, and H. Takuma, Appl. Phys. B **56**, 21 (1993).
[9] D.W. Fahey, W.F. Parks, and L.D. Schearer, J. Phys. E: Sci. Instrum. **13**, 38 (1980).
[10] K. Ohno, T. Takami, K. Mitsuke, and T. Ishidsa, J. Chem. Phys **94**, 2675 (1991).
[11] P. J. J. Tol, N. Herschbach, E. A. Hessels, W. Hogervorst, and W. Vassen, Phys. Rev. A **60**, R761 (1999).
[12] M. Kumakura, and N. Morita, Phys. Rev. Lett. **82**, 2848 (1999).
[13] A. Browaeys, J. Poupard, A. Robert, S. Nowak, W. Rooijakkers, E. Arimondo, L. Marcassa, D. Boiron, C. Westbrook, and A. Aspect, Eur.Phys.J.D **8**, 199 (2000).
[14] P. A. Molenaar, P. van der Straten, H.G.M. Heideman, and H. Metcalf, Phys. Rev. A **55**, 605 (1997).
[15] T.E. Barrett, S.W. Dapore-Schwartz, M.D. Ray, and G.P. Lafyatis, Phys. Rev. Lett. **67**, 3483 (1991).
[16] H.C. Mastwijk, M. van Rijnbach, J.W. Thomsen, P. van der Straten, and A. Niehaus, Eur. Phys. J. D. **4**, 131 (1997).
[17] F. Bardou, O. Emile, J.-M. Courty, C.I. Westbrook, A. Aspect, Europhys. Lett. **20**, 681 (1992).